Bachelor's Thesis in Electrical Engineering
Department of Electrical Engineering, Linköping University, 2022

Energy Demand and Charging Infrastructures for Electrified Urban Public Transports

Mathias Hagman

Bachelor's Thesis in Electrical Engineering
Energy Demand and Charging Infrastructure for Electrified Urban Public Transports
Mathias Hagman

LiTH-ISY-EX-ET--22/0518--SE

Supervisor:
Arvind Balachandran
ISY, Linköping University

Examiner:
Christofer Sundström
ISY, Linköping University

Division of Vehicle Systems
Department of Electrical Engineering
Linköping University
SE-581 83 Linköping, Sweden

Abstract

This thesis examines and outlines the work process of determining the energy demand for an electric bus. Furthermore, it presents three different solutions for an electrified urban transport infrastructure based on the bus routes currently in use in Linköping. The energy demand for the electric bus is determined using bus specifications from the manufacturer along with height maps of Linköping, real-time data from buses and a longitudinal vehicle model. The three different infrastructure solutions, denominated as "cases" in this thesis, provides a combination of different battery sizes, charging station locations and capacities and charging plans. The energy demand for the electric bus for the selected route is presented along with thorough explanations of the factors that affect the energy demand. The advantages and disadvantages of the suggested infrastructure solutions are discussed and the solution resulting in the smallest required battery size is presented. The thesis concludes that the third option, the Electric Road system solution is the best option for the infrastructure design due to its smaller battery size requirement and the lowered cost that it brings, along with a versatile design that can handle possible future bus route alterations.

Acknowledgments

I want to thank *Christofer Sundström*, my examiner at Linköping University for all the knowledge, encouragement and help during the work of this thesis.

I would like to thank *Arvind Balachandran*, my supervisor at Linköping University for his patience with me and always providing excellent answers and guidance through my process of writing this thesis.

I would also like to thank *Daniel Jung* at Linköping University for the advice and knowledge regarding the previous work done in Matlab.

Lastly, I would like to thank my friends and family for the support and encouragement during the work of the thesis.

Nomenclature

Abbreviation	Meaning
F_a	Aerodynamic force
F_r	Rolling resistance
F_g	Gravitational pull
F_i	Inertial force
$F_v(t)$	Force applied at the wheels
$P_v(t)$	Power applied at the wheels
P_{gen}	Motor generation power
P_m	Rated motor power
η_d	Driveline efficiency
η_c	Power converter efficiency
η_g	Gearbox efficiency
η_m	Electric motor efficiency
P_{regen}	Regenerated power
P_{dc}	Power draw for battery for propulsion
P_{HVAC}	Power consumption of HVAC
HVAC	Heating, Ventilation and Air Conditioning unit
P_{total}	Total power consumption of the vehicle
E_{total}	Total energy consumption of the vehicle
$E_{total,extreme}$	Extreme case energy consumption of the vehicle
ERS	Electric Road System
$\eta_{d,ERS}$	Driveline efficiency while traveling on the ERS
$P_{dc,ERS}$	Power draw for propulsion while traveling on the ERS
$P_{total,ERS}$	Total power consumption while traveling on the ERS
E_{bat}	Battery size
$E_{bat,extreme}$	Battery size for extreme case
DoD	Depth of Discharge
SoC	State of Charge
$P_{charger}$	Battery charger power
C_{rate}	Discharge rate of the battery
EFC	Equivalent Full Cycles
C_{day}	No of battery cycles per year

Figures

Figure 1: Geometrical relationship for the road angle α. 3
Figure 2**:** Forces acting on a vehicle in motion. 4
Figure 3: Illustration of an electric vehicle battery and its capacity distribution. 11
Figure 4: Layout of bus route 16 from Östgötatrafiken:s website 13
Figure 5: Battery capacity level during a 24-hour period for case 1. 14
Figure 6: Battery capacity level during a 24-hour period for case 2 with a detailed zoom of the fast charging at the end stop. 15
Figure 7: Battery capacity level during a 24-hour period for case 3 with midday and night-time charging marked. 16
Figure 8: Detailed figure of the battery capacity level for a segment of the day. 17
Figure 9: Roadmap of the electric bus route with the color-coded road segments plotted for the ERS case. 17
Figure 10: Plot of the bus route coordinates in longitude and latitude. 18
Figure 11: Bus route plotted on top of a geographical roadmap of Linköping. 19
Figure 12: The bus route plotted on top of the heightmap of Linköping and its surrounding areas. 20
Figure 13: The speed profile and the height profile of the bus for the drive cycle. 20
Figure 14: Distance travelled throughout the drive cycle. 24
Figure 15: Road angle throughout the drive cycle, in degrees. 24
Figure 16: Force on the vehicle throughout the drive cycle, in kN. 25
Figure 17: Power consumption during the drive cycle, in kW. 26
Figure 18: Energy consumption throughout the drive cycle for normal and extreme days. 27
Figure 19: Energy consumption comparison with/without ERS. 28
Figure 20: Comparison of number of cycles and EFC completed for the charging infrastructure cases. 29

Tables

Table 1: the 24-hour period timetable of the selected bus route 13
Table 2: Matlab Add-ons used in the thesis. 19
Table 3: Vehicle characteristics of the electric bus used in the thesis [11]. 23
Table 4: Comparison of battery size, charger size and C-rate for the charging infrastructure cases. 28

Contents

Abstract iii

Acknowledgments iv

Nomenclature v

Figures vi

Tables vi

1 Introduction 1

1.1 Motivation 1

1.2 Purpose 1

1.3 Research questions 1

2 Theory 2

2.1 Previous research 2

2.2 Distance travelled, acceleration and road angle of the drive cycle 3

2.3 Vehicle motion equation 4

2.4 Power applied at the wheels 5

2.5 Regenerative braking 6

2.6 Power consumption of HVAC 7

2.7 Total power and energy consumption of the vehicle 8

2.8 Extreme day energy consumption 8

2.9 Electric Road System 9

2.10 Battery sizing 10

2.11 Power requirement of chargers 11

2.12 Additional battery specifications 12

2.13 Electric Bus and the bus route 12

2.14 Charging infrastructure cases 13

2.14.1 Case 1, Night-time charging 14

2.14.2 Case 2, charging throughout the day 15

2.14.3 Case 3, Electric Road System 16

3 Methods 18

3.1 Prestudy 18

3.2 Distance travelled during drive cycle 21

3.3 Road angle during the drive cycle 21

3.4 Energy demand for the drive cycle 22

4 Results 23
4.1 Vehicle characteristics 23
4.2 Distance travelled during the drive cycle 24
4.3 Road angle during the drive cycle 24
4.4 Power and energy consumption of the drive cycle 25
4.5 Energy consumption while traveling on the ERS 28
4.6 Battery size, charger capacity and C-rate for the charging infrastructure cases 28
5 Discussion 30
5.1 Methods 30
5.2 Results 30
5.2.1 Battery size 30
5.2.2 Charger capacity and C-rate 31
6 Conclusion 32
6.1 Future work 32
Bibliography 33

1 Introduction

The electrification of urban transport systems has been going on for quite some time with a variety of different solution existing all over the world. The change to electrified urban transports has brought many environmental advantages by reducing the use of fossil-based fuel and enabling the limited amount of available biofuel to be utilized for longer distance transports, along with reducing the emission in the cities. By using electric vehicles, the energy efficiency has also improved and the noise level from transport has been reduced. [1]

The transition to electrified urban transports has introduced new and interesting challenges for the engineers of the world to solve. In this thesis, a basic model of an electric bus is presented, and the energy demand is determined based on said model. The energy demand lays the ground to three proposed solutions for an electric urban transport charging infrastructure in Linköping, including battery sizes and battery charger powers.

1.1 Motivation

This topic is highly relevant with today's focus on environmentally friendly transports and the electric bus with its infrastructure will be a part of the solution to a society that uses more energy efficient and renewable energy. Many publications have been published on the subject and the work presented in this thesis will outline the basic steps in determining energy demands for electric vehicles.

1.2 Purpose

The task of determining the energy demand of an electric bus and designing an urban transport system infrastructure is a big process with many variables. The purpose of this thesis is to outline the work process and establish a base for future work in the area.

1.3 Research questions

- What parameters need to be taken in consideration to determine the energy consumption of an electric bus?

- Based on the existing routes and the electric buses currently operated by Östgötatrafiken along with the existing battery charging alternatives and infrastructure solutions available today, which solution for a charging infrastructure to the electric urban public transport system in Linköping would result in the smallest battery size required for operation?

2 Theory

The theory chapter will contain an introduction to the previous research that the thesis is based on as well as the theoretical background for determining the energy demand, the battery size and battery charger power of an electric vehicle. The chapter will also include a detailed description of the bus route used in the thesis along with three different charging infrastructure cases.

2.1 Previous research

This report uses results and Matlab code based on the work done in a feasibility study labelled: "charging infrastructure for electrified public transport in Linköping". The feasibility study is a project where Linköping University with Christofer Sundström as project manager and the Swedish Energy agency, working on the behalf of the Swedish government are researching and evaluating the different possibilities and solutions for electrification of the urban public transport system.

In this report the drive cycle of the vehicle is based on an actual bus route that Östgötatrafiken operates in Linköping. One of the features that Östgötatrafiken has implemented in their buses is a positioning system. This positioning system operates at a frequency of 1 Hz and provides the following data: Timestamp, longitude, latitude, and vehicle speed. This immense amount of data is publicly accessible via a website named Trafiklab. The website provides a controlled and safe way for companies to share data by using API:s (Application Programming Interface). Trafiklab provides API:s from several different regional public transport companies in Sweden, such as: SL, Skånetrafiken, Västtrafik, Samtrafiken and Östgötatrafiken.

Parts of the thesis is based on the API data retrieved from Trafiklab. To be able to use the bus data from Trafiklab, the data needs to be converted to a format that Matlab can process. This is done by using a JavaScript that converts the API: s to Excel spreadsheets, the spreadsheets are then imported to Matlab. An overview of the methodology used in the previously mentioned feasibility study can be found in the methods chapter.

2.2 Distance travelled, acceleration and road angle of the drive cycle

The total travelled distance from a drive cycle is calculated by taking the integral of speed over time:

$$S(t) = \int_0^t v(t). \tag{1}$$

Where $S(t)$ is distance traveled, $v(t)$ is the vehicle speed and t is the timestamps throughout the drive cycle.

Similarly, the acceleration during the drive cycle can be calculated by taking the derivative of speed over time:

$$a(t) = \frac{d}{dt} \cdot v(t). \tag{2}$$

Where $a(t)$ is the acceleration of the bus.

With the distance travelled during the drive cycle calculated and height-profile determined, the road-angle α for the drive cycle can be calculated using the following equation:

$$\alpha = arctan\ \left(\frac{\Delta h}{\Delta d}\right), \tag{3}$$

where Δh and Δd represent the difference in height and distance between two time-instances, where n denotes present value and $n-1$ is the value from the previous second, see Figure 1: Geometrical relationship for the road angle α.

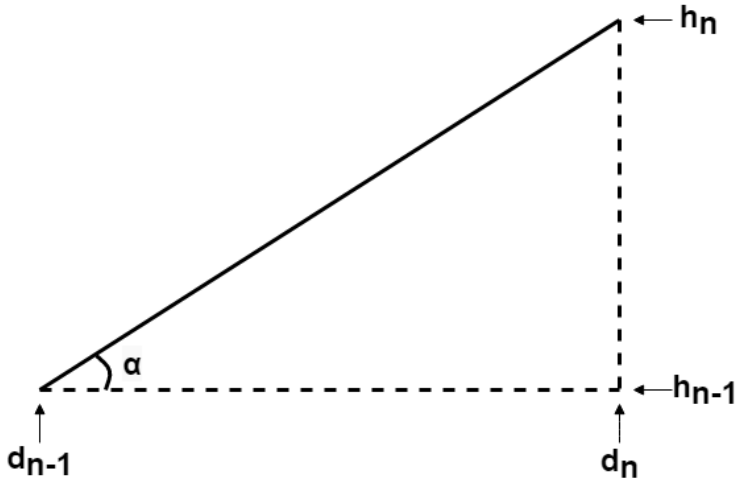

Figure 1: Geometrical relationship for the road angle α.

2.3 Vehicle motion equation

The first step in this process is to determine the force applied at the wheels of the vehicle using the *"vehicle motion equation"* [2]. The formula is designed to describe the basic forces acting on a vehicle in motion as seen below:

$$m_v \cdot \frac{d}{d(t)} v(t) = F_a + F_g + F_r + F_i, \tag{4}$$

where m_v is the mass of the vehicle $[kg]$, $v(t)$ is the speed of the vehicle $[m/s]$, F_a is the aerodynamic force $[N]$, F_r is the rolling resistance $[N]$, F_g is the force caused by gravitational pull on non-horizontal roads $[N]$ and F_i Is the inertial force $[N]$.

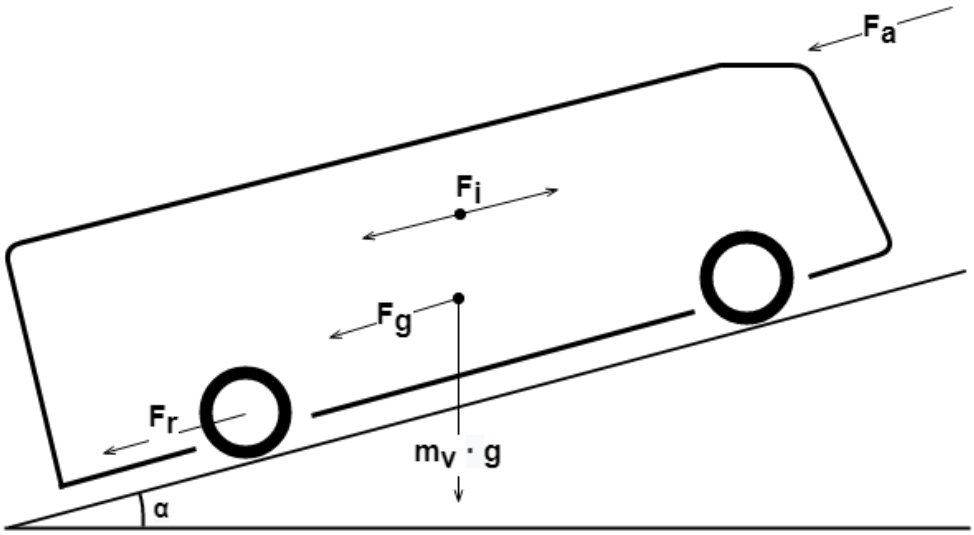

Figure 2: Forces acting on a vehicle in motion.

Aerodynamic drag force of the bus, F_a is calculated using the following equation:

$$F_a = \frac{1}{2} \cdot \rho_a \cdot A_f \cdot C_d \cdot v(t)^2, \tag{5}$$

where ρ_a is the density of air $[kg/m^3]$ and A_f is the frontal area$[m^2]$ of the vehicle, $v(t)$ is the vehicle speed $[m/s]$. The drag coefficient, C_d is dependent on many different variables such as: the shape of the vehicle body, the roughness of the surface and vehicle speed [3]. In this report the drag coefficient is considered to be constant as adopting a constant value is deemed accurate enough in the case of calculating the estimated force on the wheels of the vehicle.

The rolling resistance, F_r is calculated using the following equation:

$$F_r = C_r \cdot m_v \cdot g, \tag{6}$$

where the rolling resistance coefficient, C_r is a function of a few different variables such as vehicle speed, road surface and tire pressure to name a few. [4] Although, for many instances when the vehicle speed is somewhat normal (in this report, vehicle speed does not exceed 80 km/h) the coefficient can be assumed to be constant. m_v $[kg]$ is the vehicles mass and g $[m/s^2]$ is the acceleration due to gravitation.

Gravitational force or “uphill driving force”, F_g is determined by:

$$F_g = m_v \cdot g \cdot sin\,(\alpha), \tag{7}$$

where m_v $[kg]$ is the vehicle mass, g $[\,m/s^2]$ is the gravitational pull and $\alpha[deg]$ the road angle. The road angle is determined by the geometrical equation described in section 2.2.

The inertial force, F_i is defined as a product of the accelerating force and mass of a body acting in the opposite direction of acceleration.

Equation 8 shows the modified formula to calculate inertial force on the wheels of a vehicle:

$$F_i = (m_w + \frac{J_w}{R_w}) \cdot a, \tag{8}$$

Where m_w is the mass of the wheel $[kg]$ and a is the acceleration of the vehicle. J_w is the inertia of the wheel and is defined by the following equation: $J_w = m_w \cdot {R_w}^2$, where R_w is the radius of the wheel.

2.4 Power applied at the wheels

From basic physics we know that power equals force times speed. In this thesis the power applied at the wheels is calculated with the following equation:

$$P_v(t) = \left(m_v \cdot \frac{d}{d(t)} v(t)\right) \cdot v(t) = F_v(t) \cdot v(t), \tag{9}$$

where $P_v(t)$ is the power applied at the wheels throughout the drive cycle, $F_v(t)$ is the force on the wheels and $v(t)$ is the speed of the vehicle.

2.5 Regenerative braking

Regenerative braking in electric vehicles is the process of converting parts of the kinetic energy stored in the vehicle during deceleration to usable energy for the vehicle. The most common way of achieving this in today's electric and hybrid vehicles is by operating the motors of the vehicle as generators when the vehicle is decelerating and/or going downhill, thus generating energy that is later stored in the vehicle's battery.

The regenerative braking systems in electric vehicles varies vastly from manufacturer to manufacturer and with that the efficiency of the systems also differs, with previous research showing that regenerative braking that regenerate between 15% and 35% of the total power consumption of the vehicle. [5]

Additional to recharging the battery in the vehicle, the motors also provide braking torque to the wheels. Regenerative braking in electric vehicles can be as a serial or parallel configuration together with regular hydraulic brakes. In the serial configuration the vehicle mainly slows down with the braking torque supplied by the electric motors, and when more braking force is needed i.e., at greater speeds or steeper declines, the vehicle switches over to the hydraulic brakes. In the parallel configuration, the braking torque from the motors and the hydraulic brakes works together in tandem so that the braking torque from the electric motors increases with the hydraulic braking force. [4]

This report does not take the configuration of regenerative braking into consideration. Instead, the amount of power that the vehicle can regenerate is determined by the maximum power output of the electric motors when they are acting as generators and the efficiency of the driveline in the vehicle. When the motors are acting as generators, they cannot produce the full rated power in regeneration. In this report the regenerative output is estimated to be 90% of the rated power output of the motors, resulting in the following equation:

$$P_{gen} = 0.9 \cdot P_m, \tag{10}$$

where $P_{gen}[W]$ is the power output of the motors when they are acting as generators and $P_m\ [W]$ is the rated power output of the motors from the manufacturer spec sheet.

The driveline of electric vehicles consists of three main components: the power converter, the gearbox, and the electric motors. Thus, the total efficiency of the vehicle's driveline is defined by:

$$\eta_d = \eta_c \cdot \eta_g \cdot \eta_m, \tag{11}$$

where η_d is the total efficiency of the vehicle driveline, η_c is the efficiency of the power converter, η_g is the gearbox efficiency and η_m is the efficiency of the electric motors. In this report the efficiency of the driveline components of the vehicle in the drive cycle are not known due to limited data in the spec sheet of the vehicle. Instead, the numbers are estimations based on data found in [5]. Combining equation 10 and 11 gives us the total regenerative power of the vehicle, resulting in the following equation:

$$P_{regen} = \eta_d \cdot P_{gen}, \tag{12}$$

where $P_{regen}[W]$ is the regenerated power, η_d is the driveline efficiency and $P_{gen}\ [W]$ is the power output of the motors when they are acting as generators.

Additionally, the driveline efficiency does not only affect the amount of regenerative power flowing into the battery, but it also introduces some losses between the power drawn from the battery during acceleration and the actual power applied at the wheels.

The actual power draw from the battery to propel the vehicle is determined by the following equation:

$$P_{dc} = \frac{P_v}{\eta_d^{sgn(P_v)}}, \tag{13}$$

where P_{dc} $[W]$ is the actual power draw from the vehicle's battery to propel the vehicle, P_v $[W]$ is the power applied at the wheels and η_d is the driveline efficiency.

2.6 Power consumption of HVAC

Another component that affects the power demand and effective range of an electric vehicle is the heating, ventilation, and air conditioning unit (HVAC). The HVAC system in an electric vehicle is a complex system with designs varying vastly between manufacturers and the intended environment for the vehicle. The modelling of the HVAC systems energy consumption is a function with many factors included i.e., desired cabin temperature, outside temperature, vehicle speed, opening and closing of the bus doors, thermal energy of the passengers, auxiliary systems, and ventilation to name a few. It becomes quite clear that modelling the HVAC system and its impact on energy consumption accurately would require thorough work and could be a report in it-self. Extensive research on the subject has been done in [6].

The paper [6] simulates the power consumption of an electric bus in an urban environment and examines that the impact of traffic conditions, HVAC consumption and auxiliary consumption has and on the total power consumption of the bus. The drive cycle and the bus used in the experiment has many similarities with the drive cycle and bus used in this project. Therefore, it is deemed that the results from the paper can be used to estimate the power consumption of the HVAC system of the bus in this report. The paper provides the reader with HVAC power consumption depending on the outside temperature, both in unit of kWh/km and as a percentage of the total power consumption of the vehicle, the latter results are used in this report.

In Linköping, the average outside temperature in 2020 was eight degrees Celsius [7] and from the results in [6] this temperature would result in a power consumption of the HVAC system that is 20% of the total power consumption of the bus. The total power consumption of the HVAC system is thereby calculated by the following equation:

$$P_{HVAC} = 0.2 \cdot P_{dc}, \tag{14}$$

where $P_{HVAC}[W]$ is the total power consumption of the HVAC system and P_{dc} $[W]$ is the power drawn to propel the vehicle.

2.7 Total power and energy consumption of the vehicle

With all the factors affecting the power consumption of an electric vehicle explained and determined, the total power consumption of the vehicle is calculated with the following equation:

$$P_{total} = P_{dc} + P_{HVAC} - P_{regen}, \quad (15)$$

where $P_{total}[W]$ is the total power consumption of the vehicle throughout the drive cycle, $P_{dc}[W]$ is the

power drawn from the battery to propel the vehicle, $P_{HVAC}[W]$ is the power consumption of the HVAC system and $P_{regen}[W]$ is the regenerated power. Note that the regenerative power in equation 15 is negative since the regenerative power is flowing backwards into the battery, resulting in a smaller total power consumption.

Usually, battery sizes and energy consumption for electric vehicle are specified in units of kilowatt hours $[kWh]$. Therefore, the power consumption of the vehicle is converted to an energy consumption or as it is more commonly known, an energy demand, using the following equation:

$$E_{total}(t) = \int_{t_0}^{t} P_{total}(t) \cdot dt, \quad (16)$$

where $E_{total}(t)[kWh]$ is the instantaneous energy demand of the vehicle and $P_{total}(t)[W]$ is the instantaneous power demand of the vehicle at time instant t.

2.8 Extreme day energy consumption

Since the data that the drive cycle and the energy consumption is based on is from a day in mid-May the results is representing an average day during throughout the year. To get a more accurate representation of the changes of energy consumption over a year, an extreme day energy consumption is determined. The energy demand for extreme days is meant to represent driving conditions for some months of the year where the traction is decreased due to bad road condition (days with heavy rain, snow, winds etc.) along with a higher HVAC consumption to keep a comfortable cabin temperature, resulting in a larger energy consumption. In this thesis the energy demand for extreme days is assumed to be 20 % larger than on a normal day. Thus, the extreme days energy demand can be calculated with the following equation:

$$E_{total,extreme}(t) = E_{total}(t) \cdot 1.2, \quad (17)$$

where $E_{total,extreme}(t)[kWh]$ is the extreme days energy demand and $E_{total}(t)[kWh]$ is the energy demand of the vehicle throughout the drive cycle, calculated in equation 16.

2.9 Electric Road System

An alternative to the more traditional way of constructing an electrified urban transport system is the Electric Road System (ERS). A ERS is defined as a stretch of road where an electric vehicle can connect itself and receive electrical energy, both for propulsion and for charging the battery. The connection between the electric vehicle can vary between design but the most common ways is to connect via either overhead lines (similar to electric trains), with conductive rails or via induction (wireless connection). [8]

While the electric vehicle is traveling on the ERS, the energy demand of the vehicle changes. Since the ERS provides energy to propel the vehicle and charge the battery separately some of the drivetrain losses are reduced.

As explained in chapter 2.5 we know that the actual energy demand is larger than the energy needed at the wheels because the energy is transferred from the battery, through the converter, through the gearbox and into the electric motors.

The benefit of the ERS is that the energy to propel the vehicle goes directly into the gear drivetrain and the motors, thus the in efficiency from the battery converter is removed from the equation and the driveline efficiency while traveling on the ERS is as follows:

$$\eta_{d,ERS} = \eta_g \cdot \eta_m, \tag{18}$$

where $\eta_{d,ERS}$ is the driveline efficiency while the vehicle is traveling on the ERS, η_g is the gearbox efficiency and η_m is the efficiency of the electric motors.

The energy consumption of the electric vehicle while using the ERS is therefore determined by the following relation:

$$P_{dc,ERS} = \frac{P_w}{\eta_{d,ERS}^{sgn(\eta_{d,ERS})}}, \tag{19}$$

where $P_{dc,ERS}\ [W]$ is the actual power demand for the vehicle's propulsion, $P_w\ [W]$ is the power applied at the wheels and $\eta_{d,ERS}$ is the driveline efficiency while on the ERS.

Thus, the total power consumption of the vehicle while traveling on the ERS is defined by the following equation:

$$P_{total,ERS} = P_{dc,ERS} + P_{HVAC} - P_{regen}, \tag{20}$$

where $P_{total,ERS}[W]$ is the total power consumption of the vehicle while traveling on the ERS, $P_{dc,ERS}[W]$ is the power drawn from the ERS to propel the vehicle, $P_{HVAC}[W]$ is the power consumption of the HVAC system and $P_{regen}[W]$ is the regenerated power. Note that the HVAC and regenerative power stays the same while on the ERS.

2.10 Battery sizing

The battery size of the electric vehicle in this thesis is calculated in two stages, the first is given by the following:

$$E_{bat} = \frac{(E_{total} \cdot n)}{DoD_{window}}, \quad (21)$$

where $E_{bat}[kWh]$ is the battery size of the vehicle, $E_{total}[kWh]$ is the energy demand of the vehicle per drive cycle, n is the number of drive cycles between charging and DoD_{window} is the Depth of Discharge window.

The DoD is defined as the percentage of battery capacity discharged in relation to the initial/maximum battery capacity expressed in percent as seen in the following:

$$DoD = \frac{discharged\ capacity}{maximum\ capacity} \cdot 100\%. \quad (22)$$

The DoD-window determines the maximum and minimum allowed battery discharge. i.e. a DoD-window of 70 % means that the battery is allowed to discharge from fully charged (0% DoD) all the way down to 70 % DoD. When the battery has been discharged to 70% DoD it is considered to be empty. The DoD of a battery is directly corelated to the Batter State of Charge (SoC) as seen in the following equation:

$$DoD = 100\% - SoC, \quad (23)$$

where SoC is the state of charge in percent. The SoC of a battery in thereby an inverse of the DoD and both are valid options for describing battery levels. [9]

The second stage of battery sizing is an extreme day energy demand check, using the following equation:

$$\frac{E_{total,extreme} \cdot n}{E_{bat}} = \begin{cases} < 0.8, battery\ size\ adequite \\ > 0.8\ battery\ size\ to\ small' \end{cases} \quad (24)$$

where $E_{total,extreme}[kWh]$ is the total extreme day energy demand per drive cycle, n is the number of drive cycles between charging and 0.8 corelates to a battery DoD of 80% (up to 20% SoC).

The check is done to ensure that the selected battery capacity can handle an extreme case energy demand without discharging below 20% SoC (above 80% DoD).

The 20% percent discharge margin directly correlates to the End-of-Life (EoL) of the battery. The EoL capacity is the point at which a battery will only hold a set percentage if its initial storage capacity [10]. In this thesis the EoL percentage is set at 20%, so that when the battery only can hold 80% of its initial capacity it is considered to have reached its end of life.

If the result of equation 24 is larger than 0.8, the battery size is recalculated with the following:

$$E_{bat,extreme} = \frac{E_{total,extreme} \cdot n}{0.8}, \quad (25)$$

where $E_{bat,extreme}[kWh]$ is the battery size with capacity to handle an extreme case scenario, $E_{total,extreme}[kWh]$ is the extreme day energy demand for the drive cycle and n is the number of cycles. An illustration of the batteries in this thesis is presented in Figure 3 with the DoD-window, margin for extreme energy demand days and margin for capacity loss (EoL capacity loss) marked.

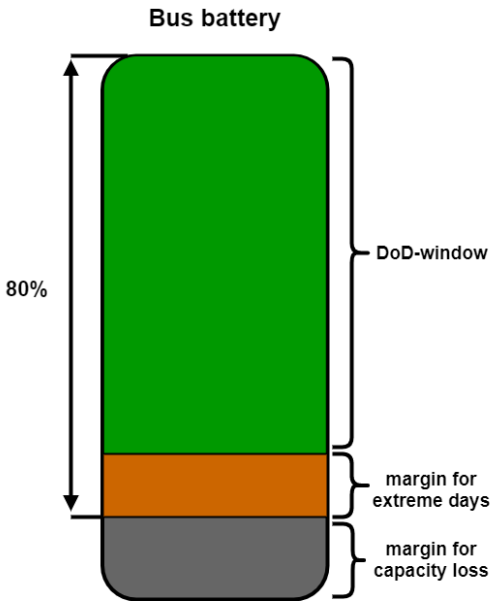

Figure 3: Illustration of an electric vehicle battery and its capacity distribution.

In this thesis, 100% battery level does not correspond to a fully charged battery, but rather a battery level of 80%. This assumption is done based on the fact that in reality, batteries are not charged to 100% or discharged fully to 0% due to the fact that the health of batteries are greatly decreased if one were to charge or discharge them to 100% and 0% respectively. This phenomenon means that most batteries in electric vehicles are a bit larger than they need to be for its intended purpose. A larger battery with its extra costs is considered an acceptable compromise for achieving longer lasting and healthier batteries.

2.11 Power requirement of chargers

The power requirement for the charging stations in the electric bus infrastructure is calculated by dividing the desired battery capacity with the available charging time, resulting in the following:

$$P_{charger} = \frac{E_{bat} \cdot DoD_{window}}{t_{charge}}, \tag{26}$$

where $P_{charger}[W]$ is the battery charger power, $E_{bat}[kWh]$ is the bus battery capacity, DoD_{window} is the DoD-window of the bus battery and $t_{charge}[hours]$ is the available charging time in hours.

2.12 Additional battery specifications

An important specification listed for batteries is the charging rate of the battery, more commonly known as the C-rate. The C-rate can be calculated by diving 1 over the charging time in hours, in this thesis in calculated by dividing the charger capacity with the battery capacity as seen in the following equation:

$$C_{rate} = \frac{1}{h} = \frac{P_{charger}}{E_{bat}} = \frac{\cancel{kW}}{\cancel{kW}h} = \frac{1}{h}, \quad (27)$$

where C_{rate} is the C-rate of the battery, $h[hours]$ is the charging time, $P_{charger}[W]$ is the power of the battery charger and $E_{bat}[kWh]$ is the battery capacity.

Another common variable that is mentioned in literatures about general battery data is Equivalent Full Cycles (EFC). The EFC is a measurement used to compare batteries with different capacities and DoD-windows. The EFC is often used by manufacturer for warranty and estimated lifetime of the battery, i.e., a battery spec sheet could say that the battery will last for x number of years with y amount of EFC:s completed. The EFC is calculated with the following equation:

$$EFC = DoD_{window} \cdot C_{day} \cdot 365, \quad (28)$$

where EFC is the Equivalent full cycles for a year and C_{day} is the total number of full cycles (fully discharge and then fully charged) per day.

2.13 Electric Bus and the bus route

The electric bus that is used in this thesis to calculate an energy demand is the Chinese brand Build Your Dream (BYD) K11, an 18-meter bus with a capacity of above 50 passengers that is currently in use in the urban traffic in Linköping [11]. The specification of the bus is presented in the results chapter. The bus route used in this thesis is route 16, the route starts at Berga centrum, traveling through the city center and into the bus and railway station, continuing out to the residentials areas east of the city center and ending at Aspnäset [12]. The route layout can be seen in Figure 4.

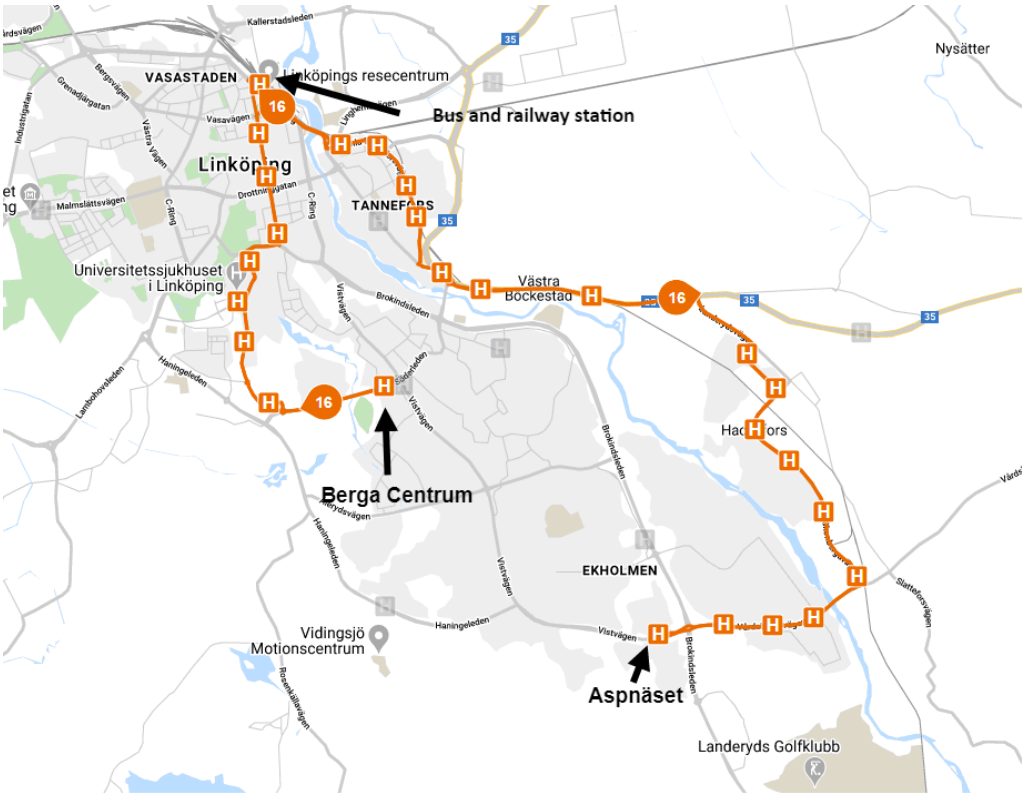

Figure 4: Layout of bus route 16 from Östgötatrafiken:s website

By studying the bus schedule from Östgötatrafiken a 24-hour driving schedule was constructed, presented in Table 1 [12].

Time window	Comment
06:00 – 12:00	Normal driving from end stop to end stop
12:00 – 14:00	Midday stop
14:00 – 24:00	Normal driving from end stop to end stop
24:00 – 06:00	Night stop

Table 1: the 24-hour period timetable of the selected bus route

2.14 Charging infrastructure cases

This thesis presents three different plausible solutions for a charging infrastructure in a future electrified public transport system in Linköping. The different solutions are in in this thesis presented as “cases” and are based on the bus model and bus route presented in the previous sub-chapter.

2.14.1 Case 1, Night-time charging

In this case the electric bus is only charged at midday between 12:00 and 14:00 and during the night, between 24:00 and 06:00. Figure 5 shows how the battery capacity level changes during a 24-hour period, the flat spots of the curve in the figure represents the 15-minute standstills at the end stops between trips.

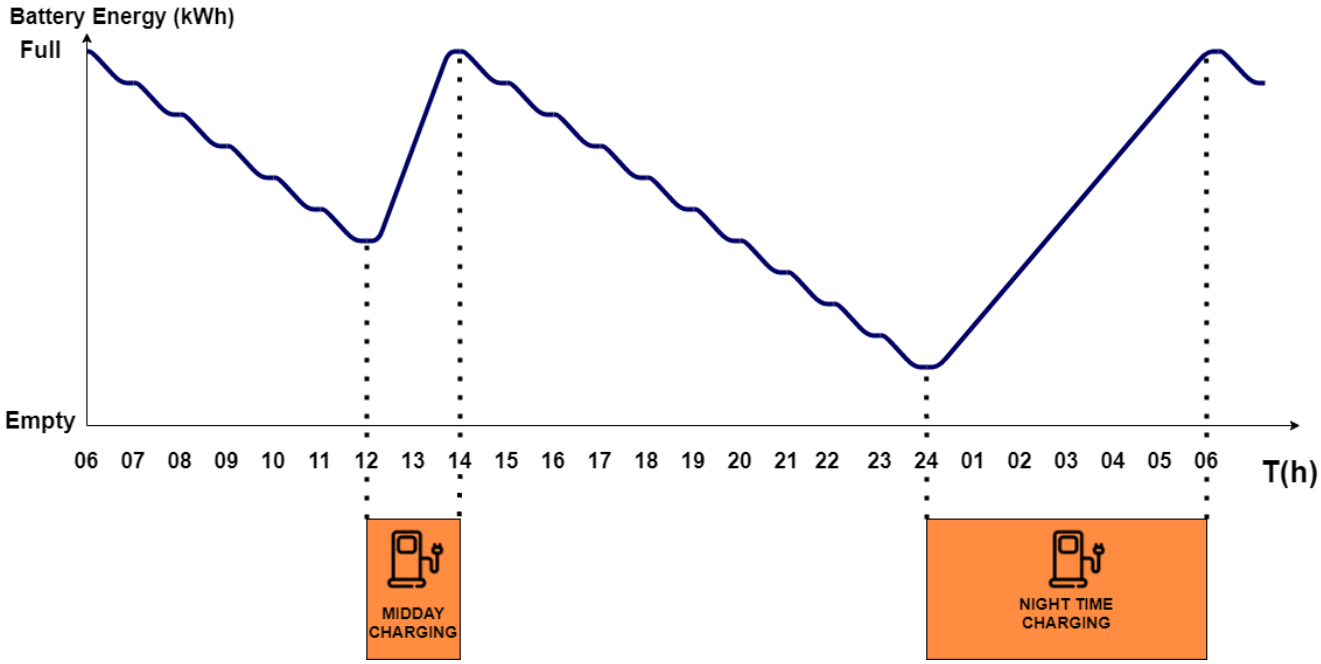

Figure 5: Battery capacity level during a 24-hour period for case 1.

2.14.2 Case 2, charging throughout the day

In case 2 the electric bus is charged at the Berga centrum end stop between trips for 15 minutes, at midday between 12:00 and 14:00 and at night between 24:00 and 06:00. The battery capacity during the day is shown in Figure 6.

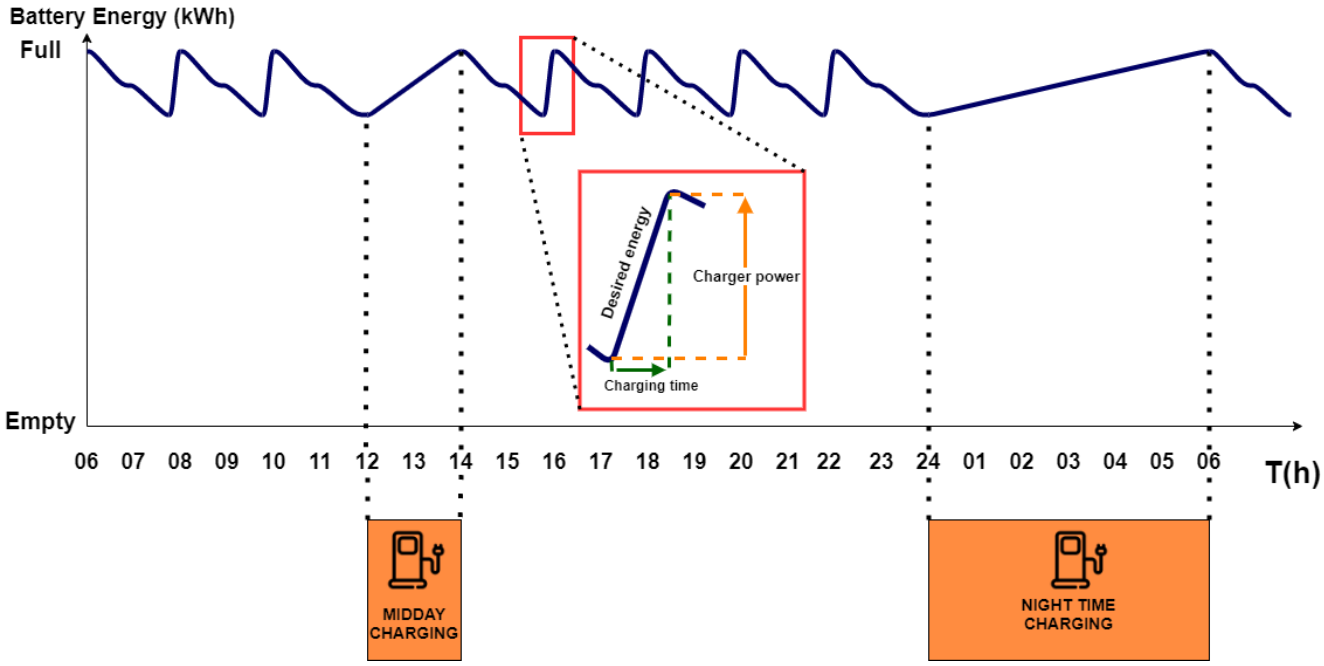

Figure 6: Battery capacity level during a 24-hour period for case 2 with a detailed zoom of the fast charging at the end stop.

2.14.3 Case 3, Electric Road System

The third case utilizes an electric road system (ERS) as explained in chapter 2.9 where the electric bus is charged while it is driving on the ERS. The bus is also charged at midday and at night similarly to the two previous cases. The battery capacity level is shown in Figure 7.

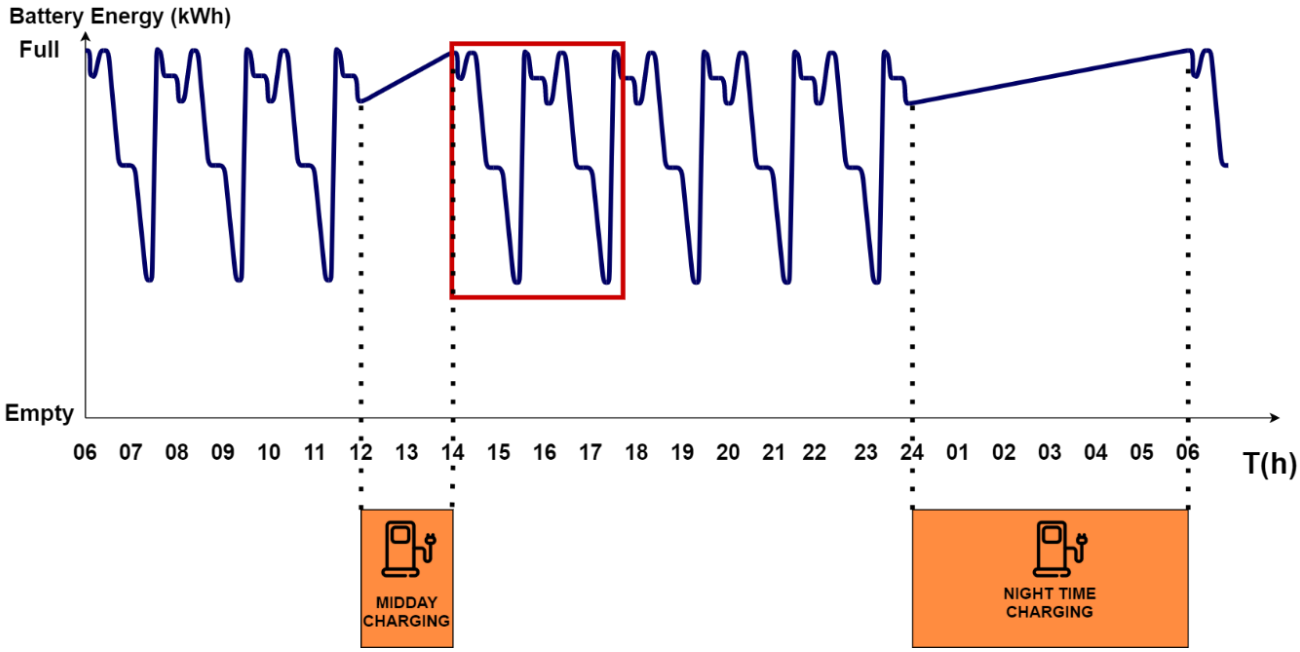

Figure 7: Battery capacity level during a 24-hour period for case 3 with midday and night-time charging marked.

A more detailed figure of the battery level (highlighted in red in Figure 7) is presented in Figure 8. To further help visualize the battery level during the day the different color-coded road segments of the trip is plotted on a map of the electric bus route in Figure 9. The ERS begins at the intersection of Sankt lars-gatan (northeast of Universitetssjukhuset) and ends at the bus and railway station, the total travel time on the ERS is 11 minutes.

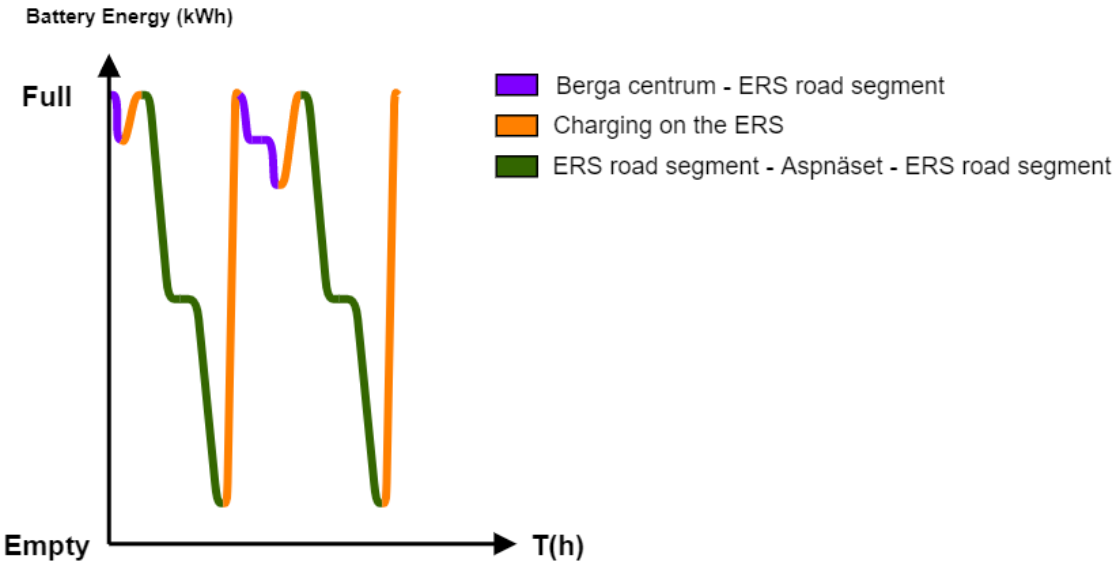

Figure 8: Detailed figure of the battery capacity level for a segment of the day.

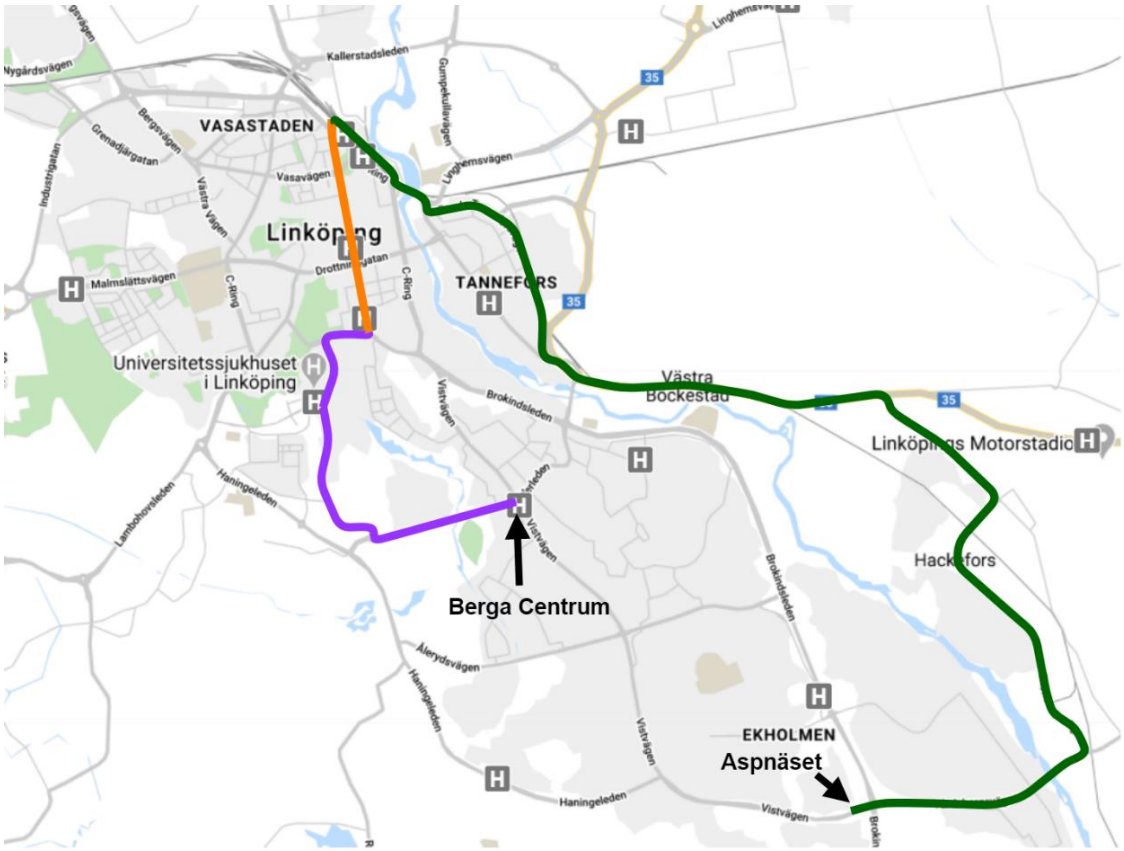

Figure 9: Roadmap of the electric bus route with the color-coded road segments plotted for the ERS case.

3 Methods

The methods chapter covers the process and methods used in the thesis to achieve the results. The chapter also includes information about the previous work that the thesis is based on.

3.1 Prestudy

The project started with getting familiar with the Matlab code and data provided by the research group explained in the theory chapter, understanding the calculations and how they could be used in the project. This was done with the help of the Matlab guides and by having meetings with some of the researchers. With the basics of the Matlab code covered the work of determining a suitable bus route began. The Trafiklab database contains data from every route that Östgötatrafiken operates, almost 130 different routes. Since this thesis only focuses on electric vehicle infrastructure in an urban environment, a bus-route for the inner city was wanted, thus route 16 was selected. Below is a simplified explanation of the given Matlab code and the results from the research group.

The bus position from route 16 was plotted onto a figure to visually study the selected bus route as seen in. The variation of the gaps between the positioning points in the figure is simply a phenomenon caused by varying vehicle speed during the drive cycle, where a larger gap between positioning points denotes a larger vehicle speed.

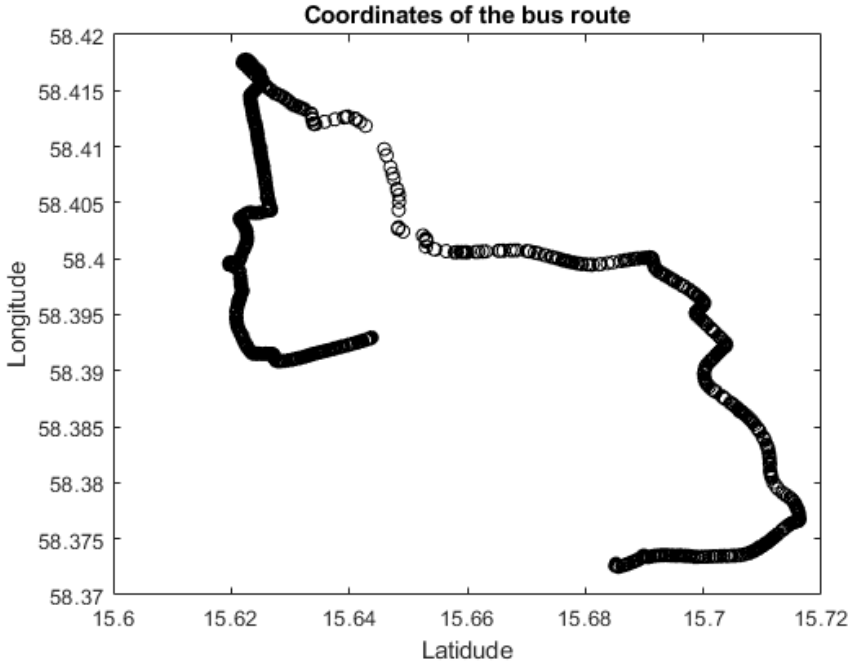

Figure 10: Plot of the bus route coordinates in longitude and latitude.

This alone might not give a good oversight of the route, especially for readers not familiar with the bus routes or the layout of Linköping in general. To remedy this, the Geoscatter function was used in Matlab. Geoscatter is part of the Mapping toolbox, a downloadable add-on for Matlab that allows users to plot coordinates onto geographical roadmaps. Table 2 shows a list of the Matlab add-ons used in the project and the bus route plotted on top of the geographical roadmap can be seen in Figure 11.

	Name	Author
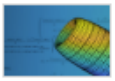	**Symbolic Math Toolbox** version 8.7	MathWorks
	**Stateflow** version 10.4	MathWorks
	**Simulink** version 10.3	MathWorks
	**Powertrain Blockset** version 1.9	MathWorks
	**Mapping Toolbox** version 5.1	MathWorks

Table 2: Matlab Add-ons used in the thesis.

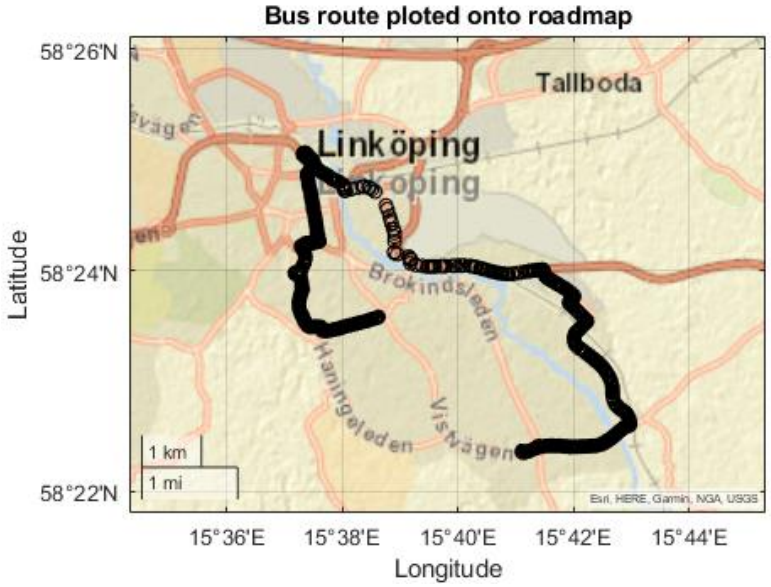

Figure 11: Bus route plotted on top of a geographical roadmap of Linköping.

Additional to the plotted bus route, a height profile of the route was determined. This was done by plotting the bus route on top of a heightmap of Linköping. The heightmap has an accuracy of around 2 meters and was acquired from Lantmäteriet, the Swedish mapping, cadastral and land registration authority. The results of plotting the bus route on top of the heightmap is presented in Figure 12, where the colours of the background represent the height of the ground above sea level in meters. The bar on the right side of Figure 12 explains the relationship between a colour and the height above sea level. The height profile along with the speed profile of the drive cycle can be seen in Figure 13, note that the sudden change to straight lines ¾ into the drive cycle seen in Figure 13 means that the bus is stopped and turned off, thus the total driving time for the drive cycle from end stop to end stop is 45 minutes.

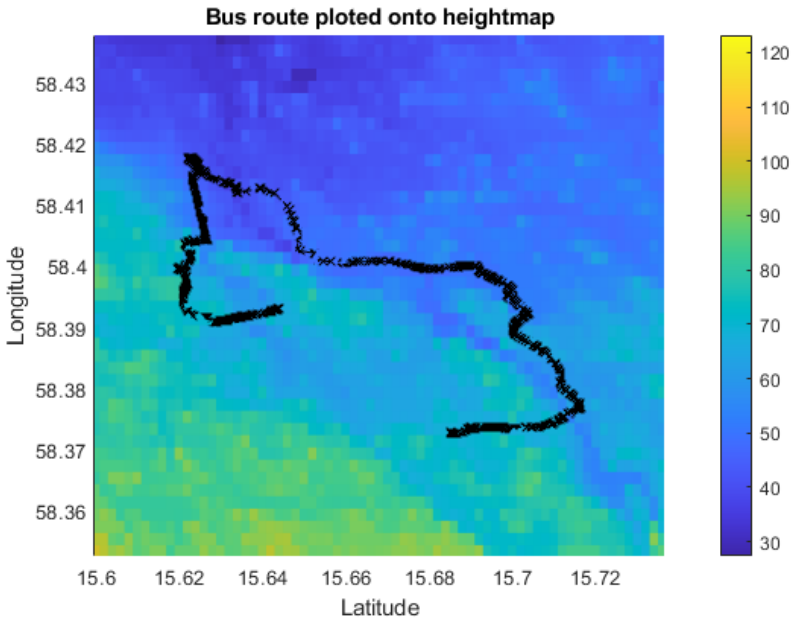

Figure 12: The bus route plotted on top of the heightmap of Linköping and its surrounding areas.

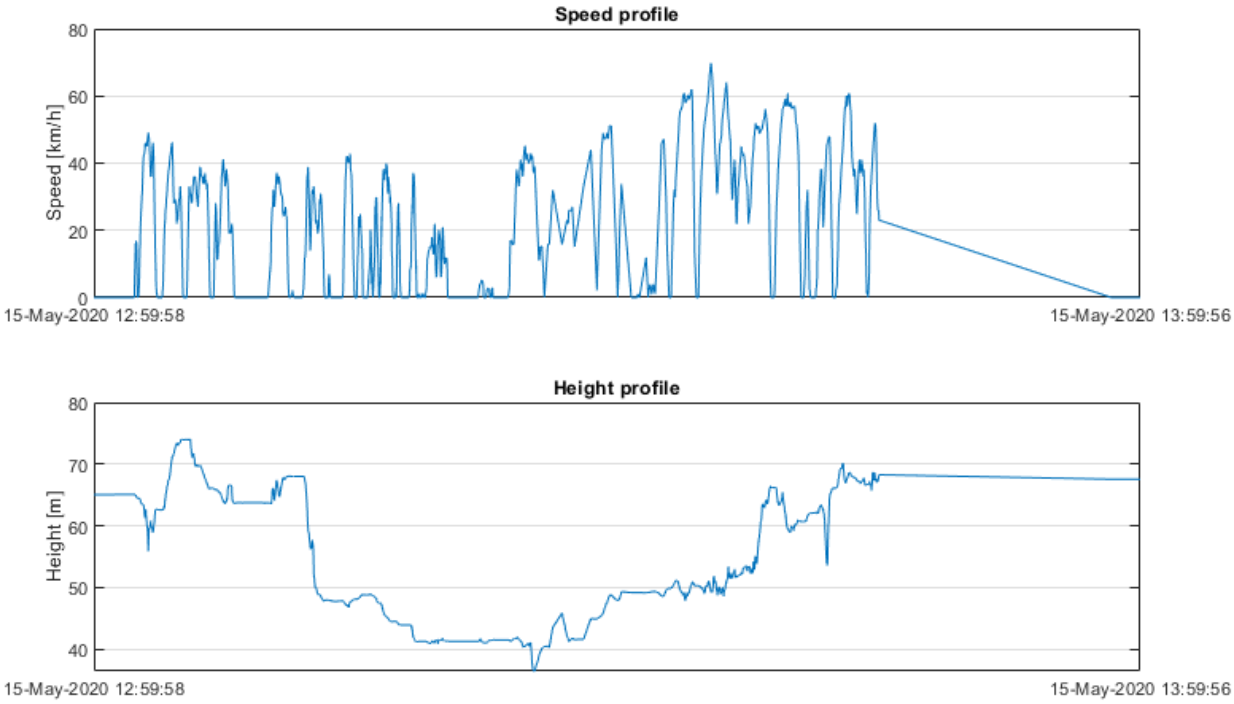

Figure 13: The speed profile and the height profile of the bus for the drive cycle.

3.2 Distance travelled during drive cycle

The travelled distance for the electric bus during the drive cycle was determined with the help of the "cumtrapz" function in Matlab as seen by the following Matlab code:

```
distance_bus = cumtrapz (bus_t, bus_v);
```

where distance_bus is the distance travelled for the electric bus, bus_t is the vector containing all the timestamps of the drive cycle and bus_v is the vector containing the electric bus speed for the corresponding timestamp. The cumptrapz function performs an integration of the vehicle speed over the vehicle timestamp. The results were then plotted in a figure with the distance travelled in kilometres on the Y-axis and the time elapsed in minutes on the X-axis with the following Matlab code:

```
Figure;
plot((bus_t-bus_t(1))/60, distance_bus/1000, 'm-' );
ylabel ('distance travelled in km');
xlabel ('time elapsed in minutes');
xlim ([0 60]);
title ('Distance travelled throughout the trip');
```

where bus_t-bus_t(1)is the current timestamp minus the timestamp of the first datapoint in the vector. The subtraction is done to ensure that the time elapsed starts at 0 minutes. The division on the timestamps by 60 is to convert the results to minutes instead of seconds, the same goes for the vehicle distance, a division by 1000 converts the travelled distance to kilometres instead of meters.

3.3 Road angle during the drive cycle

The road angle for the drive cycle is calculated in Matlab with an arctan function named "atan", the following Matlab code was used:

```
for i =2:numel(bus_v)
  h2 = bus_h(i)-bus_h(1);
  h1 = bus_h(i-1)-bus_h(1);
  d2 = distance_bus(i)-distance_bus(1);
  d1 = distance_bus(i-1)-distance_bus(1);
  alpha(i) = atan((h2-h1)/(d2-d1));
  alpha(isnan(alpha)) = 0;%replaces NaN values with a 0.
End
```

where alpha(i)is the road angle and the (i)indexing the current cell in the vector. Similarly to when the distance travelled was calculated the first datapoint is subtracted from the variables to set a starting point for the height and distance. The isnan check at the last line of the for-loop is done to ensure that the road angle vector does not contain any NaN values. A NaN value in Matlab is defined as "Not A Number" and occurs in Matlab when a calculation is done that renders a result that is undefined, i.e. division by zero or infinity.

After that, all road angels larger/smaller than +/- 40 degrees is filtered out and converted from radians to degrees with the following code:

```
alpha (alpha > +(40*pi)/180) = 0;
alpha (alpha < -(40*pi)/180) = 0;
alpha_deg = rad2deg(alpha);
```

The removal of the road angles larger/smaller than +/- 40 degrees is done based of the maximum incline/decline specifications from electric bus spec sheet along with the assumption that road angels larger than +/- 40 degrees in an urban environment are not realistic. Lastly, the road angle vector is plotted in a figure with the road angle on the Y-axis and time elapsed in minutes on the X-axis:

```
plot((bus_t-bus_t(1))/60, alpha_deg, 'r-');
ylabel('road angle in degrees');
xlabel('time in seconds');
ylim([-40 40]);
```

3.4 Energy demand for the drive cycle

The force acting on a vehicle in motion mentioned in the theory chapter is converted to a power consumption (Newtons to kW) and divided into two categories, the positive power demand for when the vehicle is accelerating or going uphill, and negative power demand for when the vehicle is slowing down or going downhill with the following Matlab script:

```
Pv= Fv .* bus_v; %convert force to power demand
Pv_dh = Pv.*(Pv<0); % negative power
Pv_uh = Pv.*(Pv>0); % positive power
```

where Pv_dh is the negative power vector and Pv_uh is the positive power vector from the drive cycle. The usable regenerative braking power is then determined by filtering out the powers larger than -270 kW (see theory chapter for explanation) from the negative energy vector with the following script:

```
Pv_dh_regen = Pv_dh.*(Pv_dh > -270*10^3);
```

Here, Pv_dh_regen is the usable regenerative power for the drive cycle and Pv_dh is the negative power vector. The actual regenerated power from the drive cycle is smaller due to the losses in the drivetrain of the electric vehicle and the drivetrain losses also introduce a larger actual power draw from the electric vehicle battery, as explained in the theory chapter. The actual regenerated power from the drive cycle is named Pv_regen and the actual power draw from the battery is named Pv_dc.

The total energy consumption from the drive cycle is determined by adding the power draw from the HVAC system, Pv_hvac with the power draw from the battery and the regenerated power (that is negative) and integrating it over the timestamp vector, resulting in:

```
% Total power for the bus during the drive cycle
Pv_sum = Pv_dc + Pv_regen + Pv_hvac;


%% Total energy in kWh
Ev_total = cumtrapz((bus_t/3600), Pv_sum); % integrate power over time
```

4 Results

The results chapter will present the results of the thesis along with tables and graphs comparing the different charging infrastructure cases.

4.1 Vehicle characteristics

Table 3 shows the vehicle characteristics of the electric bus used in the project to achieve the results.

Table 3: Vehicle characteristics of the electric bus used in the thesis [11].

Vehicle characteristics	
variable	**value**
Air density, $\boldsymbol{\rho_a}$	1.2 $[kg/m^2]$
Frontal Area, $\boldsymbol{A_f}$	8.59 $[m^2]$
Drag coefficient, $\boldsymbol{C_d}$	0.7
Vehicle speed, $\boldsymbol{v(t)}$	$0 \leq v \leq 20$ $[m/s]$
Rolling resistance coefficient, $\boldsymbol{C_r}$	0.015
Vehicle mass, $\boldsymbol{m_v}$	28 500 $[kg]$
Gravitational pull, $\boldsymbol{g}$	9.82 $[m/s^2]$
Road angle, $\boldsymbol{\alpha}$	$-40° \leq \alpha \leq 40°$
Wheel mass, $\boldsymbol{m_w}$	45 $[kg]$
Wheel inertia, $\boldsymbol{I_w}$	11.18 $[N]$
Wheel radius, $\boldsymbol{R_w}$	0.49 $[m]$

4.2 Distance travelled during the drive cycle

The travelled distance for one drive cycle is shown in Figure 14 with a total travelled distance of 15.62 kilometres. The flat spots of the graph indicate stand stills of the bus between trips.

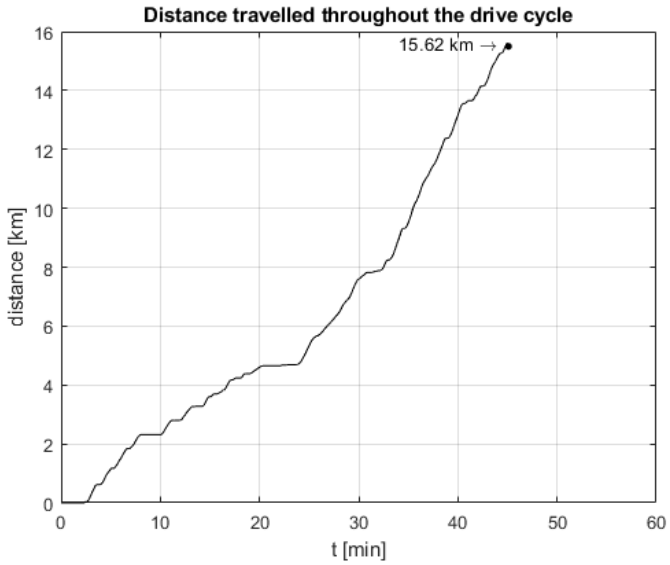

Figure 14: Distance travelled throughout the drive cycle.

4.3 Road angle during the drive cycle

Figure 15 shows the road angle of one drive cycle in degrees, the maximum road angle occurred 42 minutes into the drive cycle with an incline of 11.3 degrees. The maximum decline can be found 13 minutes into the drive cycle with an angle of −18 degrees. The height profile of the drive cycle can be found in Figure 13.

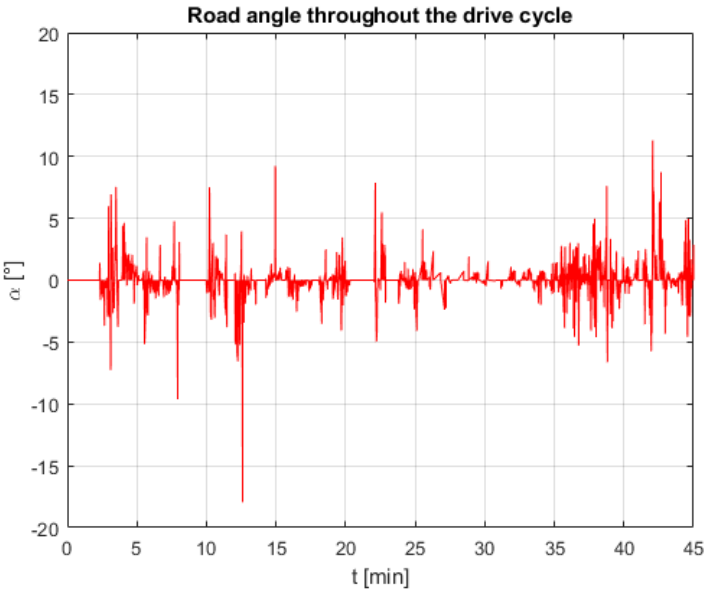

Figure 15: Road angle throughout the drive cycle, in degrees.

4.4 Power and energy consumption of the drive cycle

The force on the wheels throughout the drive cycle can be seen in Figure 16. The maximum force on the wheels is found 42 minutes into the drive cycle with a value of $59.65\ kN$, note that the maximum force on the wheels occurs at exactly the same timestamp as the largest incline throughout the drive cycle. The same relationship can be seen between the largest decline in Figure 15 and the largest negative force on the wheels, $-81.7\ kN$ in Figure 16, both occurring 13 minutes into the drive cycle.

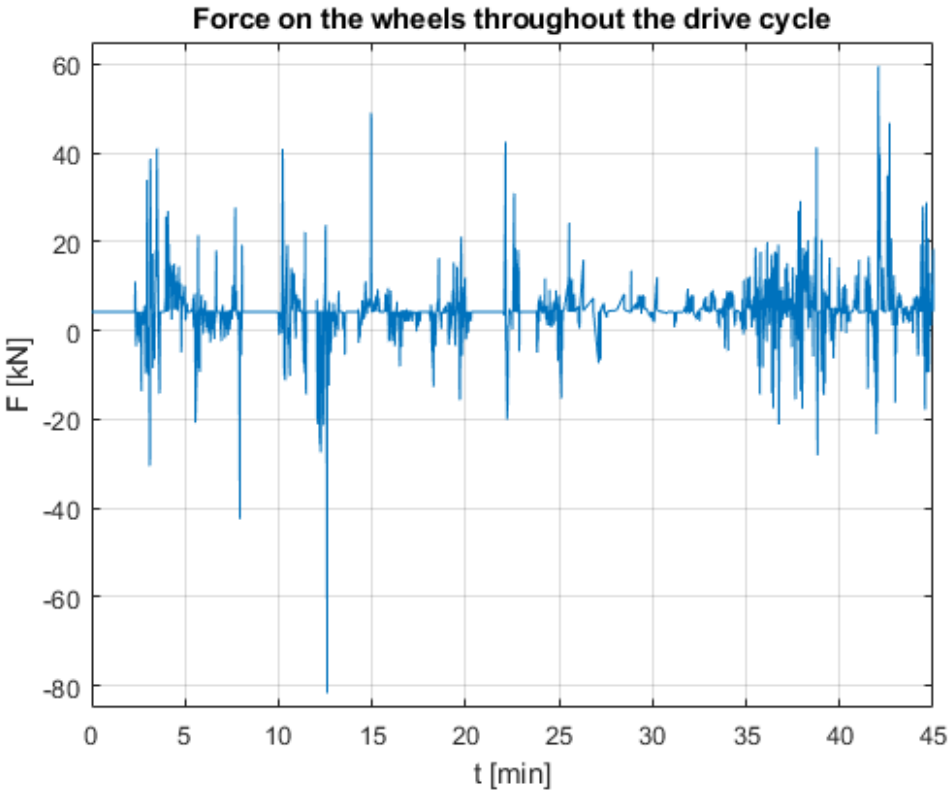

Figure 16: Force on the vehicle throughout the drive cycle, in kN.

Figure 17 shows the power consumption of the electric bus throughout the drive cycle. The maximum power consumption can be found 42 minutes into the drive cycle with a value of $1127\ kW$. The largest negative power consumption is found 38 minutes into the drive cycle with a value of $-202.8\ kW$, this is the maximum amount of regenerated energy throughout the drive cycle. The spikes in power consumptions represent the torque spikes that occur in the driveline during gear changes and is most likely enlarged due to the applied filtration of the road angle in Figure 15 that only discards road angles above and below 40 degrees.

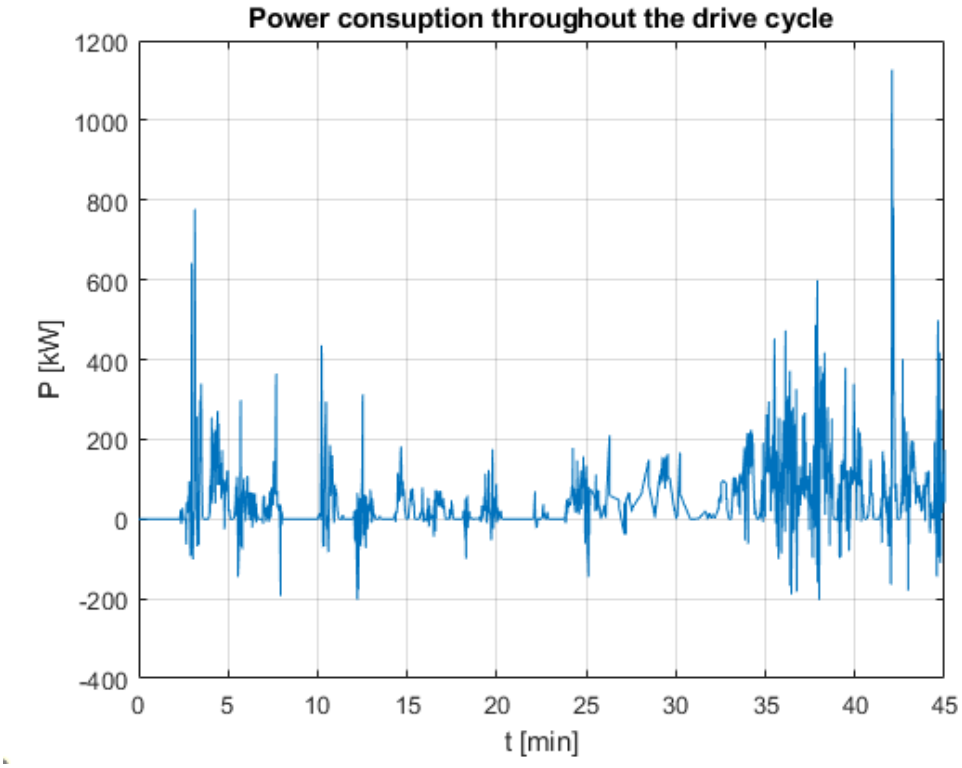

Figure 17: Power consumption during the drive cycle, in kW.

Figure 18 shows the energy consumption of the electric bus for one drive cycle. The blue line represents the energy consumption on a normal day and the red line is the energy consumption on an extreme day, explained in 2.8 Extreme day energy consumption. The total energy consumption accumulates to 33.6 kWh on a normal day, and 40.3 kWh on an extreme day.

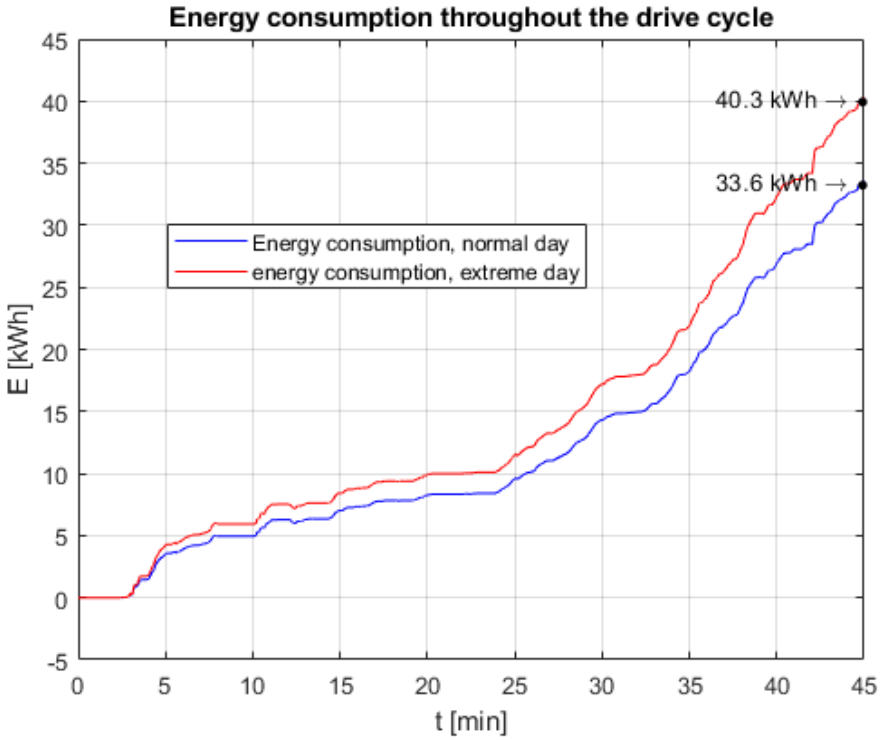

Figure 18: Energy consumption throughout the drive cycle for normal and extreme days.

4.5 Energy consumption while traveling on the ERS

Figure 19 shows the difference in energy consumption for the case when the electric bus is traveling on the same stretch of road between the intersection of Sankt lars-gatan and the bus and railway station, with the bus connected to the ERS in red, and not connected to the ERS in blue. The energy consumption for the electric bus while not connected to the ERS reaches a total of 2.26 kWh, and in the case when the electric bus is connected to the ERS the energy consumption reaches a total of 2.18 kWh.

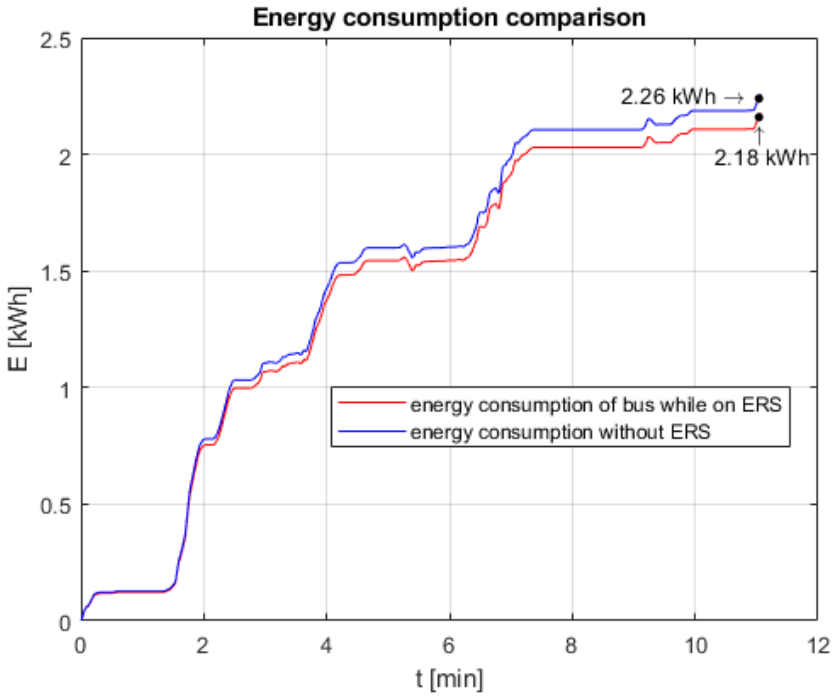

Figure 19: Energy consumption comparison with/without ERS.

4.6 Battery size, charger capacity and C-rate for the charging infrastructure cases

Table 4 shows the compilation of the battery and charger specifications for the different charging infrastructure cases. Mentionable data in the table is the end stop charger size for case 2 with a total power of 1075 kW with a corresponding C-rate of 2.4 along with the 8.4 kW night stop charger for case 3 and the corresponding C-rate of 0.08.

	Cases		
Variable	**1**	**2**	**3**
Battery size [kWh]	504	448	100
Charger, day stop [kW]	106	134	25
Charger, end stop [kW]	N/A	1075	N/A
Charger, night stop [kW]	59	45	8.4
Charger, ERS [kW]	N/A	N/A	274
C-rate, day stop	0.21	0.30	0.25
C-rate, end stop	N/A	2.40	N/A
C-rate, night stop	0.12	0.10	0.08
C-rate, ERS	N/A	N/A	2.73

Table 4: Comparison of battery size, charger size and C-rate for the charging infrastructure cases.

In Figure 20 the number of completed battery cycles and the EFC for each charging infrastructure case after 5 years of use is displayed.

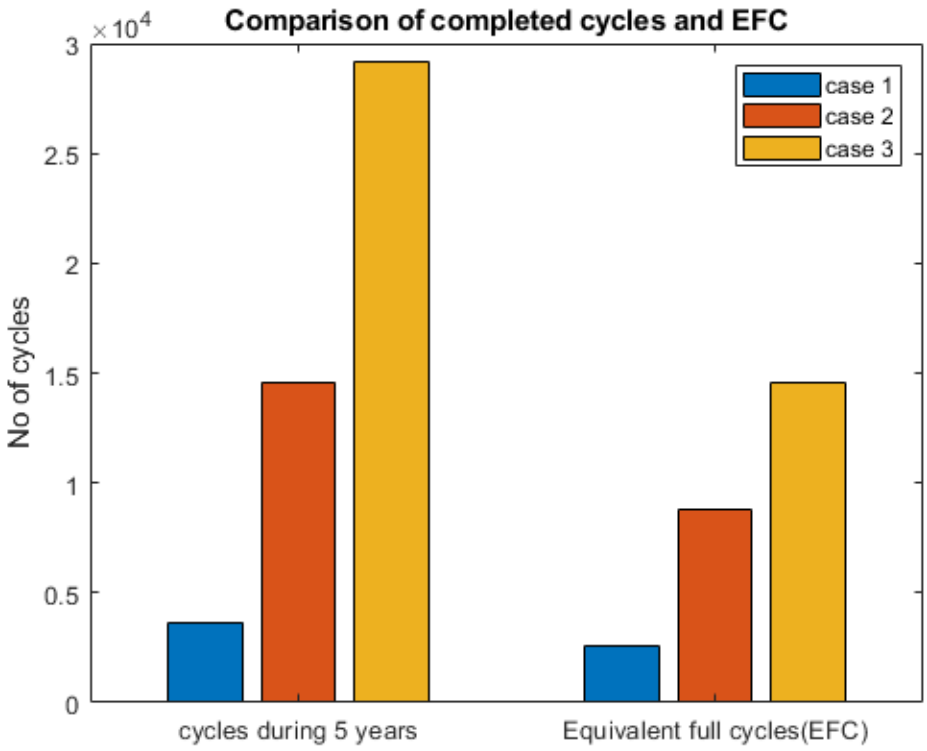

Figure 20: Comparison of number of cycles and EFC completed for the charging infrastructure cases.

5 Discussion

This chapter contains the discussion of the results and the methodology of the thesis. The majority of the problems that occurred were bugs in the MATLAB scripts or misconceptions of the theory. Since this thesis is solely theoretical there will be no discussion of any mishaps or complications during tests.

5.1 Methods

The decision to use simplified equations to calculate the Extreme day energy consumption will most likely degrade the accuracy of the total energy consumption for the electric bus. A more defined equation could have been achieved by studying the energy demand for several trips throughout the year, one per month for example. Another solution could be to reach out to the traffic operator for a collaboration to get access to energy demand data from their database. The same idea of collaboration could be utilized to achieve a more defined model for the HVAC energy consumption, taking the varying Swedish climate into consideration.

Due to the time restraints of the Thesis along with some technical issues with the Trafiklab database, the drive cycle data was only based on one trip, for one bus route. The outcome was a general, but adequate representation of the driving data of the electric bus. A more detailed representation of the bus drive cycle or "behaviour" throughout the day could be obtained by using data from different days of the year and maybe even use data from different routes to achieve a model that is applicable for all buses used in Linköping. Proposals of focus points for methods to future work is described in chapter 6.1.

5.2 Results

The majority of the results for the thesis agree with the theoretical calculations from chapter 2. Below follows discussions for parts of the results for the thesis that stood out with unexpected and interesting outcomes.

5.2.1 Battery size

The low battery size needed for case 3 is a great result in terms of cost, a smaller battery is obviously much cheaper than a large one. A smaller battery yields more battery cycles (EFC) per year that decreases the battery health and lifespan. One benefit of having smaller batteries and replacing them more frequently than a large one is the impact that development of battery technology has on the battery purchase price. Thus, buying large batteries at lower frequency could be more expensive than buying smaller sizes at higher frequency.

A benefit of having a larger battery size is the added versatility, if the bus is designed with a battery size capable of operating only a few different routes in and around the city the bus fleet becomes vulnerable to breakdowns and the need for different configurations in the bus fleet can be a large expense. The impact that battery size can have on the mobility of the bus grid can be reduced by having a well-planned infrastructure that is versatile and with little to no effect on the buses availability if the bus routes is altered in the future.

5.2.2 Charger capacity and C-rate

The large end stop charger capacity for case 2 introduces large demands on the power grid of the infrastructure, not just because of the large power demand but also the need of power cables capable of delivering said power. If the power grid needs to be upgraded to be able to handle the power demand of the charger infrastructure, the costs could grow significantly. As with all types of high-power units a charger with more capacity introduces some safety hazards. If the charger are to be placed on a bus stop in a busy city, careful planning has to go into the design of these units to ensure a safe environment for travellers and bus operators.

Generally, high C-rates (rate of 2 or more) is not great for the health and life expectancy for batteries and should be avoided if possible. The end stop charger C-rate for case 2 and the ERS C-rate for case 3 both have a C-rate larger than 2 and will have a long-term impact on the battery life of the electric bus.

6 Conclusion

The goal of the thesis was to examine and outline the work process of determining the energy demand of an electric bus used in an urban transport system, this has been described thoroughly in the theory part and used to achieve the infrastructure solutions for the electrified urban transport system. Along with energy demand calculations, the case that resulted in the smallest battery size needed in an implementation of an electrified urban transport system based on the bus routes currently in use in Linköping will be presented below.

Many factors come into play during the process of shaping the electrified urban transport infrastructure, for example if a completely new power grid needs to be laid down because of higher power delivery demands the cost for the completion of the urban transport infrastructure would increase considerably. As discussed in the previous chapter, the battery size is an important factor to consider during the infrastructure planning, how can one maximize the utilization of the buses by choosing a battery size that can be used on many different routes.

The smaller battery size yields lower service and maintenance cost for the bus fleet along with a smaller initial purchase price. With the fast development in the battery industry, batteries for electric vehicles will be even cheaper in the future, decreasing the cost impact of battery size selection for electrified urban transport systems. Another important factor for the urban transport infrastructure is the versatility of the design. By carefully selecting the capacity and layout of the charging stations one can achieve an infrastructure that can supply multiple routes with the advantage of needing a redesign if the routes were to change.

The infrastructure design of placing an ERS on a stretch of road in the city where a large percentage of buses in use pass through is the solution with the smallest required battery size of the electric bus. The ERS solution also have a great versatility if a change to the routes were to occur, it would with all likeliness not affect this part of the route where the ERS is laid down as the city center is built around the urban transport routes.

6.1 Future work

The work presented in this thesis is intended as a base for future work in the field of electrified urban transport infrastructure. Some parts of the work have been simplified due to time and resource restrains and below follows some suggestions of focus points for future work from the authors point of view.

The extreme day energy consumption is a challenging task and to achieve an accurate and precise formula, the main focus should be to gather more data of weather conditions and its impact on the driveline energy demand. The HVAC system energy demand calculations would also benefit of the refined “weather-profile”.

Another very important area that is highly interesting and one that has not theoretically been implemented in this thesis is the impact that the EFC and charging strategies (C-rate) has on battery ageing. Battery ageing is a vast and difficult process to define but with accurate driving-data from the electric bus drivelines and precise bus specifications, a realisation should be possible to realise. The last and perhaps most important future focus point would be to gather data from all the bus routes and determine an Infrastructure with a battery size that could accommodate all the different routes energy demand.

Bibliography

[1] C. Sundström, H. Alfredsson, M. Atterhall, A. Gunnarsson, D. Jung, J. Kempe, S. Malander and E. Skageström, “Feasability Study: Charging Infrastructure for Electrified Public Transport in Linköping,” 2020. [Online]. Available: https://www.energimyndigheten.se/forskning-och-innovation/projektdatabas/sokresultat/GetDocument/?id=3c7fa55b-0d07-4ff1-8488-1682d00250d0&documentName=slutrapport_buss.pdf.pdf.

[2] A. S. Lino Guzzella, Vehicle Propulsion Systems - Introduction to Modeling and Optimization, Berlin, Heidelberg: Springer, 2013.

[3] Engineering ToolBox, “The Engineering ToolBox,” 2004. [Online]. Available: https://www.engineeringtoolbox.com/drag-coefficient-d_627.html. [Accessed 01 05 2021].

[4] B. J. Varocky, “Benchmarking of Regenerative,” TNO Automotive, Helmond &, Eindhoven , 2011.

[5] A. R. N. L. Z. R. Valery Vodovozov, “Energy saving estimates for regenerative braking and downhill driving of battery electric vehicles,” in *Biennial Baltic Electronic Conference*, Tallinn, Estonia, 2014.

[6] A. Z. H. E. Z. F. Nader A. El-Taweel, “Novel Electric Bus Energy Consumption Model based on probabilistic synthetic speed profile integrated with HVAC,” *IEEE TRANSACTIONS ON INTELLIGENT TRANSPORTATION SYSTEMS,* vol. 22, no. 3, 2021.

[7] S. M. o. H. Institut, ”smhi.se,” [Online]. Available: https://www.smhi.se/data/meteorologi/kartor/arsmedeltemperatur. [Använd 18 05 2021].

[8] M. G. H. G. S. T. Håkan Sundelin, “The maturity of electric road systems,” in *2016 International Conference on Electrical Systems for Aircraft, Railway, Ship Propulsion and Road Vehicles & International Transportation Electrification Conference (ESARS-ITEC)*, Toulouse, France, 2016.

[9] D. S. W. Waag, “ScineceDirect,” Elsevier B.V, 2021. [Online]. Available: https://www.sciencedirect.com/topics/engineering/depth-of-discharge. [Accessed 01 07 2021].

[10] E. D. J. R. Brant Price, “Life cycle costs of electric and hybrid electric vehicle batteries and End-of-Life uses,” in *2012 IEEE International Conference on Electro/Information Technology*, Indianapolis, IN, USA, 2012.

[11] BYD Company Limited, “bydeurope.com,” BYD Company Limited, [Online]. Available: https://www.bydeurope.com/pdp-bus-model-18. [Accessed 23 06 2021].

[12] Östgötatrafiken, “ostgotatrafiken.se,” Östgötatrafiken, [Online]. Available: https://www.ostgotatrafiken.se/hallplats/aspnaset-linkoping. [Accessed 23 06 2021].

[13] R. V. C. A. S. S. M. V. V. Mineeshma G.R, “Component Sizing of Electric Vehicle / Hybrid Electric Vehicle subsystems using Backward modelling approach,” in *2016 IEEE International Conference on Power Electronics, Drives and Energy Systems (PEDES)*, Trivandrum, India, 2011.

[14] Östgötatrafiken, “ostgotatrafiken.se,” Östgötatrafiken, 18 08 2020. [Online]. Available: https://www.ostgotatrafiken.se/linje/16. [Accessed 23 06 2021].